J. Cent. South Univ. (2015) 22: 1427−1436
DOI: 10.1007/s11771-015-2660-1

Springer

Simultaneous hydraulic fracturing of ultra-low permeability sandstone reservoirs in China: Mechanism and its field test

REN Lan(任岚)[1], LIN Ran(林然)[1], ZHAO Jin-zhou(赵金洲)[1], YANG Ke-wen(杨克文)[2], HU Yong-quan(胡永全)[1], WANG Xiu-juan(王秀娟)[2]

1. State Key Laboratory of Oil−Gas Reservoir Geology & Exploitation, Southwest Petroleum University, Chengdu 610500, China;
2. Reservoir Evaluation Department, PetroChina Changqing Oilfield Company, Xi'an 710000, China

Abstract: Based on the impact of the stress perturbation effect created by simultaneous propagation of multiple fractures in the process of simultaneous hydraulic fracturing, a thorough research on the mechanism and adaptation of simultaneous fracturing of double horizontal wells in ultra-low permeability sandstone reservoirs was conducted by taking two adjacent horizontal wells (well Yangping-1 and well Yangping-2 located in Longdong area of China Changqing Oilfield) as field test wells. And simultaneous fracturing optimal design of two adjacent horizontal wells was finished and employed in field test. Micro-seismic monitoring analysis of fracture propagation during the stimulation treatment shows that hydraulic fractures present a pattern of complicated network expansion, and the well test data after fracturing show that the daily production of well Yangping-1 and well Yangping-2 reach 105.8 t/d and 87.6 t/d, which are approximately 9.4 times and 7.8 times the daily production of a fractured vertical well in the same area, respectively. Field test reflects that simultaneous hydraulic fracturing of two adjacent horizontal wells can enlarge the expansion area of hydraulic fractures to obtain a lager drainage area and realize the full stimulation of ultra-low permeability sandstone reservoirs in China Changqing oilfield. Therefore, simultaneous fracturing of two adjacent horizontal wells provides a good opportunity in stimulation techniques for the efficient development of ultra-low permeability reservoirs in China Changqing oilfield, and it has great popularization value and can provide a new avenue for the application of stimulation techniques in ultra-low permeability reservoirs in China.

Key words: Changqing Oilfield; ultra-low permeability; simultaneous fracturing; double horizontal wells

1 Introduction

In recent years, under the impetus of multiple stage fracturing technology of horizontal well [1−3], USA achieved leapfrog development in the exploitation of unconventional natural gas in ultra-low permeability shale reservoirs; the annual output was 878×10^8 m^3 in 2009 while it increased to 1720×10^8 m^3 by 2011, which was an amazing output growth. Micro-seismic monitoring map of hydraulic fracture propagation in shale reservoirs showed that hydraulic fracture propagation in shale reservoir presented a pattern of fracture network expansion [4−7]. Some studies have confirmed that the effect of fracturing will be better with the increase of stimulated reservoir volume (SRV) [8−9]. Thus, improving SRV became an important goal to optimize in the fracturing design of shale reservoir, and multistage step-by-step fracturing and simultaneous fracturing of horizontal wells and many other kinds of stimulation technologies were put forward successively to improve the stimulation volume and the stimulation extent of shale reservoir [10−12]. Based on the concept of SRV in shale reservoir, a larger breakthrough in the stimulation of other unconventional reservoirs, such as coal-bed methane (CBM), tight gas and shale oil, has been achieved [13−15]. China owns rich unconventional oil and gas resource [16−18], but the exploration and exploitation technology of unconventional reservoirs has just started, especially reservoir stimulation technique still in the stage of exploration and test [19−23]. Although some low permeability sandstone gas reservoirs represented by Sulige gas reservoir in Changqing oilfield and Xujiahe gas reservoir in Sichuan oilfield are effectively developed through stimulation [24−25], it is still in the traditional concept of fracturing

Foundation item: Project(51404204) supported by the National Natural Science Foundation of China; Project(20135121120002) supported by Specialized Research Fund for the Doctoral Program of Higher Education of China; Project(2014QHZ005) supported by Scientific Research Starting Projecting of SWPU, China
Received date: 2014−02−23; **Accepted date:** 2014−09−05
Corresponding author: REN Lan, PhD; Tel: +86−13880716361; E-mail: renlanswpu@163.com

technology to carryout on the design and implementation. In order to achieve a greater breakthrough in the development of ultra-low permeability sandstone reservoirs in China Changqing oilfield, based on the idea of the stress perturbation effect created by hydraulic fractures in the process of simultaneous fracturing for shale gas development, Changqing oilfield carried out the field test to explore new technology and new methodology of ultra-low permeability reservoir stimulation. Taking the layer of Chang-7_2 as the target reservoir, two horizontal wells (Yangping-1 and Yangping-2) were drilled in Longdong area of China Changqing oilfield. At the same time, well Yangce-1, well Yangce-2 and well Yangce-3 were drilled between the double horizontal wells as micro-seismic observation wells.

2 Principle of simultaneous hydraulic fracturing

Simultaneous hydraulic fracturing means that multiple hydraulic fracturing treatments are simultaneously performed on corresponding adjacent horizontal wells to stimulate one section shared by all fractured wells through multiple sets of fracturing equipments [12]. The essence of this technology is that the stress interference between fractures created by simultaneous fracturing of two horizontal wells is utilized to promote fractures complexity while fractures propagate in the opposite direction, and the object is to make hydraulic fractures expand into fracture network and improve the level and scope of SRV, which ultimately provides a high-speed flow channel for reservoir fluid [22].

In the process of fracturing, if the reservoir horizontal stress difference is small, especially under the influence of natural fracture, hydraulic fracture tends to propagate along the direction of natural fracture, which results in the formation of fracture network [26−29]. During simultaneous fracturing, the opened hydraulic fracture creates an induced stress field around itself and the simultaneous propagation of multiple fractures strengthens the induced stress in overlying area [12], which changes the value and direction of the initial stress field and affects the mode of fracture propagation. Therefore, the first step for simultaneous fracturing analysis is to recognize the impact of stress disturbance induced by the simultaneous propagation of multiple hydraulic fractures during fracturing. Figure 1 shows the spatial structure of horizontal wellbores, propagating hydraulic fractures and induced stress superimposed area for simultaneous hydraulic fracturing of adjacent horizontal wells.

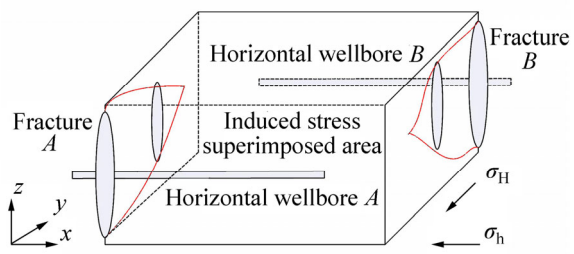

Fig. 1 Space plan of wellbore, propagating fracture and induced stress superimposed area for simultaneous hydraulic fracturing of adjacent horizontal wells

2.1 Induced stress analysis

Based on the distribution of induced stress field and propagating fracture in Fig. 1, Fig. 2 shows the plane graph for calculation of induced stress of 2-D vertical fracture in Cartesian coordinates.

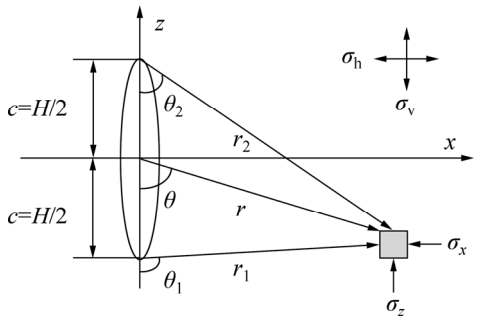

Fig. 2 Cartesian coordinates of induced stress calculation for 2-D vertical fracture

Based on the elasticity mechanics theory, and combining with Fig. 2, the stress field induced by hydraulic fracture is obtained [30] as

$$\Delta\sigma_x = p\left\{\frac{r}{\sqrt{r_1 r_2}}\cos\left(\theta-\frac{\theta_1+\theta_2}{2}\right)+\frac{c^2 r}{\sqrt{(r_1 r_2)^3}}\sin\theta\sin\left[\frac{3}{2}(\theta_1+\theta_2)\right]-1\right\} \quad (1)$$

$$\Delta\sigma_z = p\left\{\frac{r}{\sqrt{r_1 r_2}}\cos\left(\theta-\frac{\theta_1+\theta_2}{2}\right)-\frac{c^2 r}{\sqrt{(r_1 r_2)^3}}\sin\theta\sin\left[\frac{3}{2}(\theta_1+\theta_2)\right]-1\right\} \quad (2)$$

$$\Delta\tau_{zx} = p\left\{\frac{c^2 r}{\sqrt{(r_1 r_2)^3}}\sin\theta\cos\left[\frac{3}{2}(\theta_1+\theta_2)\right]\right\} \quad (3)$$

$$\Delta\sigma_y = \nu(\Delta\sigma_x+\Delta\sigma_z) \quad (4)$$

where p is net pressure, H is fracture height, and c is

fracture half-height. The relationship among geometric parameters is written as

$$\begin{cases} r=\sqrt{x^2+z^2} \\ r_1=\sqrt{x^2+(z+c)^2} \\ r_2=\sqrt{x^2+(z-c)^2} \end{cases} \tag{5}$$

$$\begin{cases} \theta=\tan^{-1}(x/-z) \\ \theta_1=\tan^{-1}[x/(-z-c)] \\ \theta_2=\tan^{-1}[x/(-z+c)] \end{cases} \tag{6}$$

Original stress field is disturbed by induced stress field created by hydraulic fractures A and B. The induced stress along the initial minimum horizontal principal stress direction in the stress superposition area is as follows:

$$\Delta\sigma_x(T)=\Delta\sigma_x(A)+\Delta\sigma_x(B) \tag{7}$$

where the induced stress $\Delta\sigma_x(A)$ and $\Delta\sigma_x(B)$ are created by fracture A and fracture B in the initial minimum horizontal principal stress direction, respectively; $\Delta\sigma_x(T)$ is the sum of the two induced stress in the initial minimum horizontal principal stress direction.

As the same, in stress superposition area, induced stress along the initial maximum horizontal principal stress direction is obtained as

$$\Delta\sigma_y(T)=\Delta\sigma_y(A)+\Delta\sigma_y(B) \tag{8}$$

where the induced stress $\Delta\sigma_y(A)$ and $\Delta\sigma_y(B)$ are created by fracture A and fracture B in the initial maximum horizontal principal stress direction, respectively; $\Delta\sigma_y(T)$ is the sum of the two induced stress in the initial maximum horizontal principal stress direction.

The horizontal induced stress difference in the initial minimum and maximum principal stress direction is defined as

$$\Delta\sigma=\Delta\sigma_x-\Delta\sigma_y \tag{9}$$

By the above calculation model of induced stress, analysis is conducted for studying the impact of hydraulic fracture on the stress field. In terms of Fig. 1, assuming that only fracture A causes stress perturbation, the horizontal induced stress difference of the initial minimum and maximum principal stress direction is shown in Fig. 3. As can be seen from Fig. 3, the induced stress difference is positive. Hence, the induced stress in the initial minimum principal stress direction is greater than the induced stress in the initial maximum principal stress direction, which can cause the horizontal stress difference becoming smaller or the change of principal stress direction under extreme conditions. And we can see that induced stress difference is weakened with the increase of the distance away from fracture A.

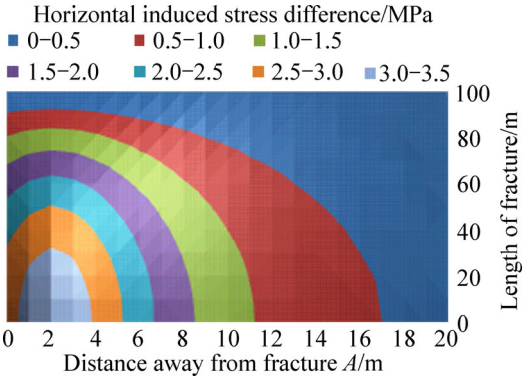

Fig. 3 Variation of induced stresses for single fracture with distance away from fracture A

Assuming that stress perturbation is caused by both fractures A and B, the induced stress is shown in Fig. 4. Compared with Fig. 3, under the effect of double fractures, the area and extent influenced by induced stress increase relative to single fracture. Hence, induced stress of double fractures has more important impact on propagation of fracture network.

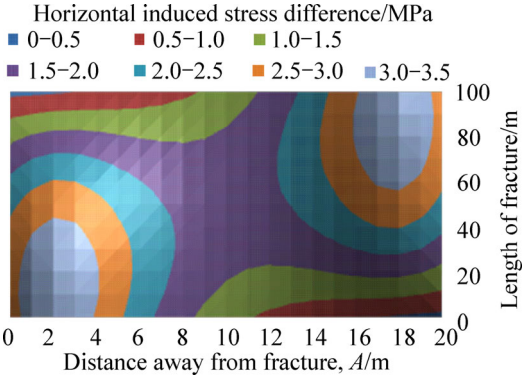

Fig. 4 Variation of induced stresses for double fractures with distance away from fracture A

2.2 Mechanics condition of fracture network expansion

For naturally fractured reservoir, it is the essential factor for the realization of fracture network expansion and reservoir stimulation that hydraulic fracture activates natural fractures [22]. Based on Warpinski criterion that is widely used for fracture propagation in naturally fractured reservoir at present [26], tensile fracture will happen to natural fracture when the fluid pressure at natural fracture overcomes the normal stress imposed on natural fracture [19]:

$$p(t)>\sigma_n+\Delta p_{nf}(t) \tag{10}$$

where σ_n is the normal stress imposed on the surface of natural fracture. According to the two-dimensional linear elastic theory, there is

$$\sigma_{\mathrm{n}}=\frac{\sigma_{\mathrm{H}}+\sigma_{\mathrm{h}}}{2}-\frac{\sigma_{\mathrm{H}}-\sigma_{\mathrm{h}}}{2}\cos(2\theta) \tag{11}$$

where σ_{H} is the maximum horizontal principal stress; σ_{h} is the minimum horizontal principal stress; θ is the angle between the maximum horizontal principal stress and natural fracture strike; $\Delta p_{\mathrm{nf}}(t)$ is the fluid pressure drop in natural fracture [31]:

$$\Delta p_{\mathrm{nf}}(t)=\frac{4\left[p(t)-p_0\right]}{\pi}\sum_{n=0}^{\infty}\frac{1}{2n+1}\cdot \exp\left[-\frac{(2n+1)^2\pi^2 k_{\mathrm{nf}}t}{4\phi_{\mathrm{nf}}\mu C_{\mathrm{t}}L_{\mathrm{f}}^2}\right]\sin\frac{(2n+1)\pi}{2} \tag{12}$$

where p_0 is the initial fluid pressure in natural fracture; L_{f} is the length of natural fracture; μ is fluid viscosity; C_{t} is the compressibility of natural fracture; ϕ_{nf} is the porosity of natural fracture; and k_{nf} is the permeability of natural fracture.

The fluid pressure at natural fracture can be expressed as the function related to net pressure:

$$p(t)=\sigma_{\mathrm{h}}+p_{\mathrm{net}}(t) \tag{13}$$

where p_{net} is the net pressure in natural fracture.

By substituting Eqs. (11) and (13) into Eq. (10), tensile fracture of natural fracture needs the net pressure:

$$p_{\mathrm{net}}(t)>\frac{\sigma_{\mathrm{H}}-\sigma_{\mathrm{h}}}{2}\left[1-\cos(2\theta)\right]+\Delta p_{\mathrm{nf}}(t) \tag{14}$$

According to Warpinski criterion, shear fracture will occur when the shear stress imposed on the surface of natural fracture is greater than the shear strength of the fracture surface.

$$|\tau|>\tau_{\mathrm{o}}+K_{\mathrm{f}}\left[\sigma_{\mathrm{n}}-p(t)\right] \tag{15}$$

where τ_0 is the cohesive force of natural fracture, K_{f} is the friction coefficient on the surface of natural fracture, and τ is the component of the shear stress imposed on the surface of natural fracture, which can be expressed as

$$\tau=\frac{\sigma_{\mathrm{H}}-\sigma_{\mathrm{h}}}{2}\sin(2\theta) \tag{16}$$

By substituting Eqs. (11), (13) and (16) into Eq. (15), shear fracture of natural fracture needs the net pressure:

$$p_{\mathrm{net}}(t)>\frac{1}{K_{\mathrm{f}}}\left[\tau_{\mathrm{o}}+\frac{\sigma_{\mathrm{H}}-\sigma_{\mathrm{h}}}{2}(K_{\mathrm{f}}-\sin(2\theta)-K_{\mathrm{f}}\cos(2\theta))\right] \tag{17}$$

Equations (14) and (17) indicate that the needed net pressure reaches the maximum when hydraulic fracture is vertical to natural fracture for any kind of fracture mode [21]. The maximum net pressure for tensile fracture is $(\sigma_{\mathrm{H}}-\sigma_{\mathrm{h}})+\Delta p_{\mathrm{nf}}(t)$, and the maximum net pressure for shear fracture is $\tau_{\mathrm{o}}/K_{\mathrm{f}}+(\sigma_{\mathrm{H}}-\sigma_{\mathrm{h}})$, which shows that above both equations are positively correlated to the horizontal stress difference. Therefore, reducing initial horizontal stress difference helps to activate natural fracture and extend fracture network fully.

Considering the combined action of initial stress and induced stress, the maximum net pressure for tensile fracture is

$$p_{\mathrm{net}}(t)_{\max}=\sigma_{\mathrm{H}}-\sigma_{\mathrm{h}}-\left(\Delta\sigma_x(T)-\Delta\sigma_y(T)\right)+\Delta p_{\mathrm{nf}}(t) \tag{18}$$

Similarly, the maximum net pressure for shear fracture is

$$p_{\mathrm{net}}(t)_{\max}=\tau_{\mathrm{o}}/K_{\mathrm{f}}+\sigma_{\mathrm{H}}-\sigma_{\mathrm{h}}-\left(\Delta\sigma_x(T)-\Delta\sigma_y(T)\right) \tag{19}$$

According to Eqs. (18) and (19), net pressure for breakdown of natural fracture will reduce because the induced stress difference in the two directions of initial horizontal principal stress is greater than zero.

$$\Delta\sigma_x(T)-\Delta\sigma_y(T)>0 \tag{20}$$

According to Eqs. (18) and (19), when the horizontal induced stress difference is equal to the initial horizontal stress difference, we can see that net pressure for the breakdown of natural fracture will decrease to minimum:

$$\Delta\sigma_x(T)-\Delta\sigma_y(T)=\sigma_{\mathrm{H}}-\sigma_{\mathrm{h}} \tag{21}$$

By transposition, the following equation is available.

$$\Delta\sigma_x(T)+\sigma_{\mathrm{h}}=\sigma_{\mathrm{H}}+\Delta\sigma_y(T) \tag{22}$$

Equation (22) indicates that it is easy for natural fracture to breakdown when the current stress field is isotropic under the effect of induced stress.

When the horizontal induced stress difference is greater than the initial horizontal stress difference, namely,

$$\Delta\sigma_x(T)-\Delta\sigma_y(T)>\sigma_{\mathrm{H}}-\sigma_{\mathrm{h}} \tag{23}$$

By transposition, the following equation is available.

$$\Delta\sigma_x(T)+\sigma_{\mathrm{h}}>\sigma_{\mathrm{H}}+\Delta\sigma_y(T) \tag{24}$$

At this time, the current horizontal stress field will reverse, and the extension direction of hydraulic fracture will thoroughly turn to the initial minimum horizontal principal stress direction, which is most favorable to the expansion of fracture network.

Based on the above analysis, when the initial horizontal stress difference in reservoir is smaller and the difference between induced stresses is greater, Eqs. (21) and (23) are more easily satisfied. So it is easier to

realize the re-orientation extension of hydraulic fracture. Figure 4 shows that, compared with the induced stress difference caused by a single fracture, the induced stress difference caused by double fractures of simultaneous fracturing is larger, then the influence scope and extent on reservoir stress field increase, which makes it easier for fracture network to expand in reservoir and has a positive effect on improving the scope and extent of SRV.

3 Geological adaptability analysis of simultaneous fracturing

The geological factors that influence fracture propagation include reservoir physical property, rock composition, rock mechanics characteristics, horizontal stress field and the distribution of natural fractures [32]. In the section, whether simultaneous fracturing is adaptive to reservoir Chang-7_2 will be discussed by taking well Yangping-1 and well Yangping-2 as pilot test wells.

3.1 Reservoir physical property

Laboratory tests on the rock cores from observation wells (well Yangce-1, well Yangce-2 and Yangce-3) were conducted. The measured average porosity and average permeability are respectively 8.72% and 0.124 mD, which shows that the physical property of reservoir Chang-7_2 is poor. For the typical ultra-low permeability reservoir, a better stimulation effect can be obtained by fracture network stimulation [22].

3.2 Natural fractures

The natural fractures in ultra-low permeability sandstone reservoirs in Longdong area can be divided into structural fractures and diagenetic fractures, as shown in Fig. 5 [33]. The average linear density of high angle fractures on rock cores is 1.25 m^{-1}; the fracture height is less than 2.2 m, mainly within 60.0 cm. The extension length of single fracture in the plane is 2.0 to 16.0 m, and the maximum length can be more than 20.0 m. The fracture development in reservoir Chang-7_2 was studied by the imaging logging on well Yangce-2. The study shows that natural fractures have developed in the reservoir, and their inclined angles range from 56° to 88°, thus they belong to middle-higher angle fracture; natural fracture trend is 34° to 276°, and ranges from north east to south west. The natural fractures in the target reservoir have an important influence on the expansion of hydraulic fracture network.

3.3 Rock constituents and mechanics parameters

The rock brittleness is controlled by rock constituents [34]. As the brittle mineral content increases, the rock brittleness becomes stronger, and it becomes easier to form fracture network under the function of outside force [35]. According to the research results of shale, the brittle mineral content more than 40% is the precondition for the formation of fracture network. The mineral content of reservoir Chang-7_2 in Longdong is dominated by both fine particle lithic feldspar sandstone and feldspar lithic sandstone, in which the content of quartz and feldspar siliceous reaches 60.7%, so the rock constituents are conducive to the formation of fracture network.

Rock mechanics parameters have great influence on the mode of fracture propagation. RICKMAN et al [36] believed that fractures tend to form fracture network in the reservoir whose rock brittleness index is more than 50.

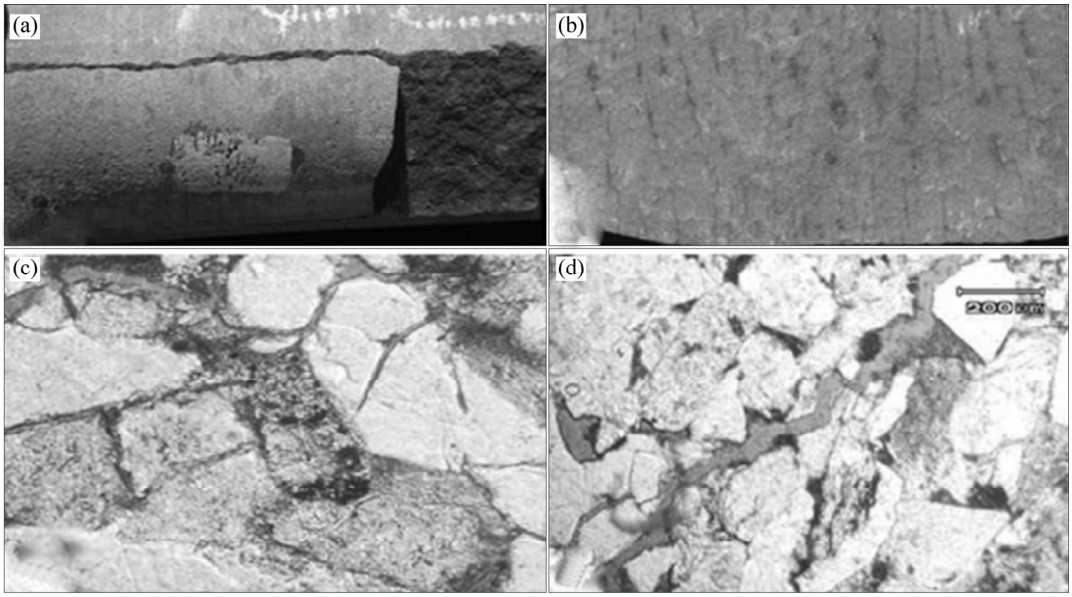

Fig. 5 Natural fractures of reservoir Chang-7_2 in Longdong area: (a) Structural fractures; (b) Diagenetic fractures; (c) Intragranular fractures; (d) Intergranular fractures

According to laboratory triaxial rock mechanics tests, average elasticity modulus is 2.98×10^4 MPa and average Poisson ratio is 0.196. The rock brittleness index is calculated as 54.9, so the rock mechanical property has a positive effect on fracture network expansion.

3.4 Reservoir stress field

According to the study on reservoir stress with paleomagnetic method and differential strain analysis, the horizontal stress distribution of reservoir Chang-7_2 in Longdong area is relatively smooth. And the horizontal stress difference is small, which ranges from 2.7 MPa to 4.0 MPa and the average value is 3.46 MPa. Experiments also show that the maximum horizontal principal stress is in the direction of north by east 70.4° to 76.1°. Horizontal wellbores in field were drilled along the direction of about north by east 160°, which is almost the same as the minimum horizontal principal stress direction, so that the main hydraulic fractures are orthogonal to the horizontal wellbore.

As can be seen from the above analysis of the geological adaptability of simultaneous hydraulic fracturing, reservoir Chang-7_2 possesses the geological conditions for simultaneous fracturing. And because of the shallow burial depth about 2100 m, there are a lot of available operating techniques to choose, such as mechanical packer staged fracturing, hydraulic jet staged fracturing, which ensures the feasibility of carrying out simultaneous hydraulic fracturing process.

4 Optimization design of simultaneous fracturing

Based on the mechanism of simultaneous fracturing and the basic reservoir characteristics above, in this section, the key parameters of simultaneous fracturing of two adjacent horizontal wells and the materials of fracturing treatment will be optimized.

4.1 Operation pumping rate

The induced stress difference created by hydraulic fracture ranges from 2.45 MPa to 3.81 MPa when net pressure is 5 MPa, and the current horizontal stress difference varies from −0.35 MPa to 1.01 MPa, which means that the horizontal stress difference is negative in some area where the stress direction reverses. In order to guarantee the full stimulation of the reservoir, the net pressure about 5 MPa should be taken into consideration to carry on the design of fracturing treatment. There is a very good positive correlation relationship between operation pumping rate and net pressure. When operation pumping rate reaches 5 m^3/min, net pressure reaches more than 5 MPa in 44% of propagating fracture; when operation pumping rate reaches 6 m^3/min, net pressure reaches more than 5 MPa in 51% of propagating fracture. Considering the influence of the simultaneous propagation of multiple fractures on net pressure, the pumping rate should be determined in the range of 6 to 8 m^3/min.

4.2 Perforation spacing

Although the fractures interaction is enhanced when perforations spacing becomes smaller, the width of fracture network zone decreases. As perforation spacing increases, the width of fracture network zone increases, but the fracture interaction is weakened, which leads to the deficient lateral extension of fracture network, then the density of fracture network decreases. Assuming that operation net pressure is 5 MPa, corresponding to different perforation spacing, the current horizontal stress difference in the middle of perforations and its reduction rate when compared with the initial horizontal stress difference are listed in Table 1. When perforation spacing is less than 20 m, the reduction rate of the horizontal stress difference is over 50%; but the reduction rate is about 50% when perforation spacing is equal to 25 m. Combining with the initial horizontal stress difference, perforation spacing should be determined between 20 to 25 m to carry on the design, including the spacing between perforation clusters in single segment of horizontal well and the spacing between cross perforations in the target segment of simultaneous fracturing of double adjacent horizontal wells.

Table 1 Influence of perforation spacing on differential horizontal stresses

Perforation spacing/m	Horizontal stress difference in middle of perforations/MPa	Reduction rate of horizontal stress difference/%
10	−1.64	147
20	1.11	67.9
25	1.80	47.9
30	2.24	35.2
40	2.73	21.0
50	2.98	13.8

4.3 Perforation parameters

In order to ensure the operability and convenience of the process implementation, hydraulic jet staged fracturing for horizontal well, which has been applied in Changqing oilfield [37], was chosen as the optimal process to accomplish the simultaneous fracturing treatment. Pressure drop caused by nozzle can be expressed as follows [38].

$$p_{\mathrm{b}}=\frac{513.559Q^2\rho}{A_{\mathrm{T}}^2C^2} \tag{24}$$

where p_b is pressure drop caused by nozzle; Q is jetting displacement, L/s; ρ is fluid density, A_T is total area of nozzle; C is the flow coefficient of nozzle.

The pressure drop of double spray gun with 8 nozzles (the diameter of each nozzle is 6 mm) is 13.77 to 30.98 MPa when the flow rate is 2.0 to 3.0 m^3/min. This double-spray gun can meet the needs of two-cluster simultaneous fracturing in single segment. Assuming that tri-spray gun has been taken to carry on the design, jetting pressure drop is 21.51 MPa, but the friction of tube increases almost half of the former, the operation pressure of the furthest fracture section reaches approximately 72.3 MPa. Considering that a large number of perforation clusters in each section would lead to the increase of operation difficulty, the scheme of double-spray gun and double-perforation clusters in each section was employed in field tests.

4.4 Fracture conductivity

Figure 6 shows the simulative annual cumulative production of single well with different major fracture conductivity. When the main fracture conductivity reaches 10 D·cm, the production growth becomes slow and gradually stabilized. Therefore, the main fracture conductivity should be designed in the range of 10 D·cm to 15 D·cm.

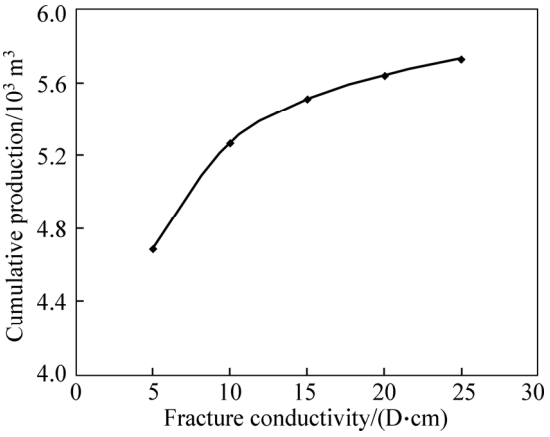

Fig. 6 Variation of annual cumulative production with major fracture conductivity

4.5 Fracturing materials

As fracturing fluid viscosity reduces, the complexity of fracture network expansion increases [39]. Therefore, the fracturing fluid of linear gel or slickwater was chosen as the main treatment fluid which prompted the forepart network expansion. Laboratory tests for the optimization evaluation of linear gel and slickwater were conducted about reservoir Chang-7_2, and the results indicated that slick water with 0.1% resistance-reducing agent did the minimum harm to reservoir, thus slick water with low damage was adopted. At the same time, in order to meet the design requirements of the main fracture conductivity in later stage, gelled fracturing fluid was adopted to carry sands so that the main fracture can be fully filled.

The chief drawback of slick water is the low capacity of transporting proppant [40]. Therefore, it is regarded as the optimization principle to choose light proppant with a small size for the branching fractures. Due to the closure stress of the reservoir Chang-7_2 in 35−40 MPa, small size of quartz sand can meet the design requirements. Thus, quartz sand of 40/70 mesh (197/355 μm) was chosen as the forepart proppant; for the filling of main fracture, small ceramsite of 30/60 mesh (250/560 μm) was used for trailed sand.

4.6 Liquid volume of fracturing treatment

Because there was no suitable simulation tool to confirm the relationship between the volume of fracturing fluid and the stimulated reservoir volume, the fracturing fluid volume design for the fracturing of shale reservoir was referred as the scale design of the field test [12], and the optimized fluid volume of each section was 600 to 800 m^3.

5 Field implementation and analysis of simultaneous fracturing

5.1 Operation basic situation

The field test of simultaneous hydraulic fracturing was performed on well Yangping-1 and well Yangping-2. Reservoir Chang-7_2 ranges in depth from 2150 m to 2250 m, and the horizontal section length of each horizontal well is approximately 1500 m. The two horizontal wells were respectively divided into 13 stages to carry out multistage simultaneous fracturing through hydraulic jet. And the combination process of abrasive perforating and fracturing treatment was simultaneously performed at two jetting points of interval about 20 m in each section. Operation parameters of the two wells are listed in Table 2. The total volume of fluid injected into each section is 455.2−834.7 m^3, and the average value is 587.2 m^3; the total volume of fluid injected into well Yangping-1 is 7794.4 m^3, while the total injection volume of well Yangping-2 is 7472.1 m^3. The amount of sand injected into each section is 37.1 to 42.2 m^3, and the average value is 39.7 m^3; the total volume of sand injected into well Yangping-1 is 519.9 m^3, while it is 515.0 m^3 in well Yangping-2. The pumping rate of tubing varies from 2.5 m^3/min to 2.8 m^3/min, while the pumping rate of casing ranges from 3 m^3/min to 4.5 m^3/min; the total pumping rate is 5.5 to 8 m^3/min. The proppant concentration ranges from 6.8% to 12.6%, and the average value is 9.33%. The operation pressure of tubing varies from 29.9 MPa to 53.9 MPa, while the operation pressure of casing ranges from 25.4 MPa to 36.5 MPa;

Table 2 Actual parameters of fracturing operation for wells Yangping-1 and Yangping-2

Well	Volume of fluid injected into each section/m^3	Volume of sand injected into each section/m^3	Tubing operation pumping rate/($m^3 \cdot min^{-1}$)	Casing operation pumping rate/($m^3 \cdot min^{-1}$)	Tubing operation pressure/MPa	Casing operation pressure/MPa	Tubing shut-in pressure/MPa	Casing shut-in pressure/MPa	Average proppant concentration/%
Yangping-1	480.6−834.7	37.1−42.2	2.5−2.8	3.0−4.5	29.9−53.9	26.3−36.5	12.6−16.4	11.7−15.5	7.9−12.6
Yangping-2	455.2−834.0	38−42.2	2.5	3.5−4.5	36.6−51.3	25.4−32.1	13.6−15.6	13.5−15.4	6.8−11.9

the shut-in pressure of casing is 11.7 to 15.5 MPa, while the shut-in pressure of tubing is 12.6 MPa to 16.4 MPa.

5.2 Analysis of fracturing treatment

According to the micro-seismic monitoring data of fracture propagation in the simultaneous fracturing performed on well Yangping-1 and well Yangping-2, the stimulated reservoir horizontal area (SRHA) of the hydraulic fractures in different sections are shown in Figs. 7 and 8, respectively. The minimum SRHA and the maximum SRHA of well Yangping-1 are respectively 1.342×10^4 m^2 and 4.674×10^4 m^2, and the total SRHA is 36.537×10^4 m^2; for well Yangping-2, the minimum value and the maximum value of SRHA are respectively 1.485×10^4 m^2 and 4.674×10^4 m^2, and the total SRHA is 35.2585×10^4 m^2. Although the stimulation extent of each section is great different from others', on the whole, the full stimulation for reservoir Chang-7_2 is realized.

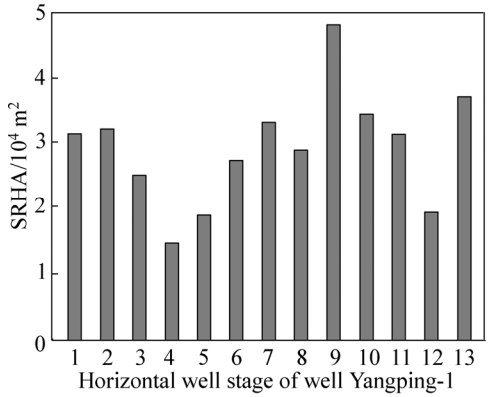

Fig. 7 SRHA of well Yangping-1 for different horizontal well stages

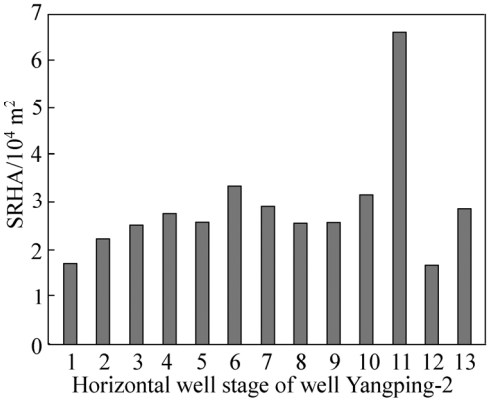

Fig. 8 SRHA of well Yangping-2 for different horizontal well stages

Figure 9 shows the relationship between the injected fluid volume and the SRHA in different sections for well Yangping-1 and well Yangping-2. There are two fracturing sections where the injected fluid volume is more than 800 m^3, but the SRHA is not the biggest; similarly, there are two fracturing sections where the SRHA is larger than 4×10^4 m^2, but the injection volume is about 480 m^3. The above shows that there is a poor correlation between the injected fluid volume and the SRHA.

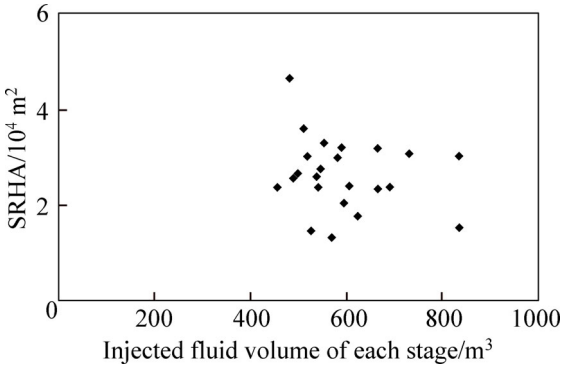

Fig. 9 Variation of SRHA with injected fluid volume

Figures 10 and 11 show the fracture network horizontal width (FNHW) of different fracturing sections of well Yangping-1 and well Yangping-2, respectively. By respectively comparing Fig. 7 and Fig. 10, Fig. 8 and Fig. 11, it can be found that the FNHW and the SRHA have a good positive correlation, that is, as FNHW increases, the SRHA increases. For the stimulation of ultra-low permeability reservoirs in the field test by

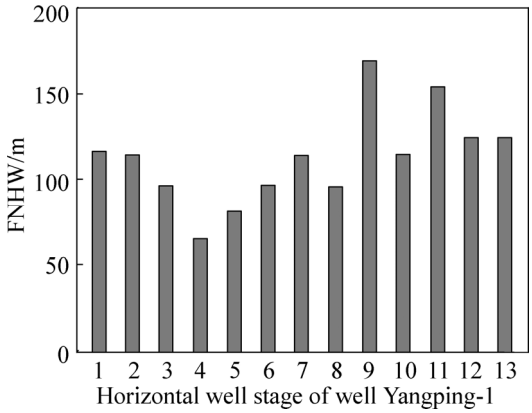

Fig. 10 FNHW of well Yangping-1 for different horizontal well stages

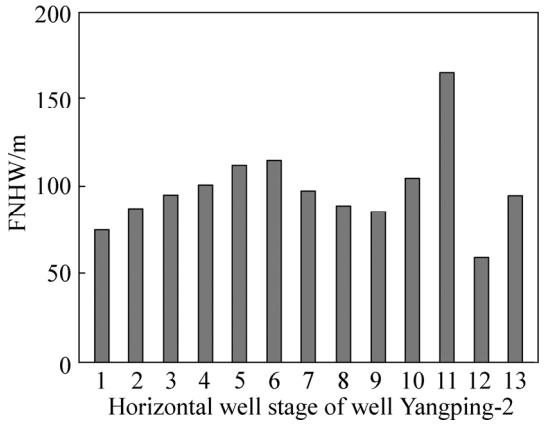

Fig.11 FNHW of well Yangping-2 for different horizontal well stages

simultaneous hydraulic fracturing of adjacent horizontal wells, broadening the FNHW is an effective way to improve the SRHA and SRV.

5.3 Evaluation after fracturing

During the production test after fracturing, the daily production of well Yangping-1 and well Yangping-2 reached 105.8 t/d and 87.6 t/d, and the two wells were respectively approximately 9.4 times and 7.8 times the daily production of a fractured vertical well in the same oil field area, which reflected that ultra-low permeability sandstone reservoirs were fully stimulated by simultaneous hydraulic fracturing of two adjacent horizontal wells, and the fracture network provided a good flow channel for reservoir fluid. The remarkable fracturing effect showed that the field test obtained a great success.

6 Conclusions

1) An in-depth research on the mechanism of simultaneous hydraulic fracturing is performed, which shows that the essential reason why simultaneous fracturing of double horizontal wells can influence the fracture network expansion is the perturbation effect and the superimposed effect of induced stress created by hydraulic fractures simultaneously extending along the opposite direction on the original stress field.

2) Based on the geologic condition of the target reservoir Chang-7_2 of the field test wells in Changqing oilfield, the adaptability of simultaneous fracturing to Chang-7_2 is analyzed, which shows that the rock crushability is outstanding, the horizontal stress difference is small, the natural fractures exist and the buried depth is shallow. The above factors indicate that it is possible for fracture network to form and expand in the reservoir. Thus, the reservoir Chang-7_2 can carry out simultaneous fracturing.

3) The fracturing practice shows that the stimulation effect of simultaneous hydraulic fracturing is remarkable. Combining with the micro-seismic monitoring data analysis, it is identified that the fracture network fully stimulated the reservoir and enlarged the drainage volume of the reservoir fluid, which shows that it is feasible to select and carry out this technological measure. For this kind of ultra-low permeability reservoirs in Changqing oilfield, simultaneous hydraulic fracturing has great popularization value and application prospect.

References

[1] EAST L E, GRIESER W, MCDANIEL B W, JOHNSON B, JACKSON R, FISHER K. Successful application of hydrajet fracturing on horizontal wells completed in a thick shale reservoir [C]// The Society of Petroleum Engineers (SPE) Eastern Regional Meeting. Charleston: SPE, 2004: 193−210.

[2] MILLE B, PANEITZ J, MULLEN M, MEIJS R, TUNSTALL M, GARCIA M. The successful application of a compartmental completion technique used to isolate multiple hydraulic-fracture treatments in horizontal Bakken shale wells in North Dakota [C]// The SPE Annual Technical Conference and Exhibition. Denver: SPE, 2008: 3992−4002.

[3] CIPOLLA C L, LOLON E P, CERAMICS C, MAYERHOFER M J, WARPINSKI N R. Fracture design considerations in horizontal wells drilled in unconventional gas reservoirs [C]// The SPE Hydraulic Fracturing Technology Conference. Woodlands: SPE, 2009: 366−375.

[4] FISHER M K, WRIGHT C A, DAVIDSON B M, GOODWIN A K, FIELDER E O, BUCKLER W S, STEINSBERGER N P. Integrating fracture mapping technologies to optimize stimulations in the Barnett shale [C]// The SPE Annual Technical Conference and Exhibition. San Antonio: SPE, 2002: 975−981.

[5] FISHER M K, HEINZE J R, HARRIS C D, DAVIDSON B M, WRIGHT C A, DUNN K P. Optimizing horizontal completion techniques in the Barnett shale using microseismic fracture mapping [C]// The SPE Annual Technical Conference and Exhibition. Houston: SPE, 2004: 1−11.

[6] MAXWELL S C, URBANCIC T I, STEINSBERGER N, ZINNO R. Microseismic imaging of hydraulic fracture complexity in the Barnett shale [C]// The Annual Technical Conference and Exhibition. San Antonio: SPE, 2002: 965−973.

[7] URBANCIC T I, MAXWELL S C. Microseismic imaging of fracture behavior in naturally fractured reservoirs [C]// The SPE/ISRM Rock Mechanics Conference. Irving: SPE, 2002: 1−7.

[8] MAYERHOFER M J, LOLON E P, YOUNGBLOOD J E, HEINZE J R. Integration of microseismic fracture mapping results with numerical fracture network production modeling in the Barnett shale [C]// The SPE Annual Technical Conference and Exhibition. San Antonio: SPE, 2006: 1−8.

[9] MAYERHOFER M J, LOLON E P, WARPINSKI N R, CIPOLLA C L, WALSER D, RIGHTMIRE C M. What is stimulated reservoir volume? [C]// The SPE Shale Gas Production Conference. Fort Worth: SPE, 2010: 89−98.

[10] SOLIMAN M Y, EAST L, AUGUSTINE J. Fracturing design aimed at enhancing fracture complexity [C]// The SPE Europec/EAGE Annual Conference and Exhibition. Barcelona: SPE, 2010: 1−20.

[11] EAST L, SOLIMAN M Y, AUGUSTINE J. Methods for enhancing far-field complexity in fracturing operations [C]// The SPE Annual

Technical Conference and Exhibition. Florence: SPE, 2010: 1−17.
[12] WATERS G, DEAN B, DOWNIE R, KERRIHARD K, AUSTBO L, MCPHERSON B. Simultaneous hydraulic fracturing of adjacent horizontal wells in the Woodford shale [C]// The SPE Hydraulic Fracturing Technology Conference. Woodlands: SPE, 2009: 1−22.
[13] CRAMER D D. Stimulating unconventional reservoirs: Lessons learned, successful practices, areas for improvement [C]// The SPE Unconventional Reservoirs Conference. Keystone: SPE, 2008: 1−19.
[14] ILK D, CURRIE S M, BLASINGAME T A. Production analysis and well performance forecasting of tight gas and shale gas wells [C]// The SPE Eastern Regional Meeting. Morgantown: SPE, 2010: 1−15.
[15] WANG Jian-wei, LIU Yang. Well performance modeling in Eagle Ford shale oil reservoir [C]// The SPE North American Unconventional Gas Conference and Exhibition. Woodlands: SPE, 2011: 1−9.
[16] JIA Cheng-zao, ZHENG Min, ZHANG Yong-feng. Unconventional hydrocarbon resources in China and the prospect of exploration and development [J]. Petroleum Exploration and Development, 2012, 39(2): 129−136. (in Chinese)
[17] ZOU Cai-neng, ZHANG Guang-ya, TAO Shi-zhen, HU Su-yun, LI Xiao-di, LI Jian-zhong, DONG Da-zhong, ZHU Ru-kai, YUAN Xuan-jun, HOU Lian-hua, QU Hui, ZHAO Xia, JIA Jin-hua, GAO Xiao-hui, GUO Qiu-lin, WANG Lan, LI Xin-jing. Geological features, major discoveries and unconventional petroleum geology in the global petroleum exporation [J]. Petroleum Exploration and Development, 2010, 37(2): 129−145.(in Chinese)
[18] HU Wen-rui, ZHAI Guang-ming, LI Jing-ming. Potential and development of unconventional hydrocarbon resources in China [J]. Engineering Science, 2010, 12(5): 25−30. (in Chinese)
[19] REN Lan. Mechanism of fracture-network fracturing for naturally fractured reservoirs [D]. Chengdu: South West Petroleum University, 2011. (in Chinese)
[20] LEI Qun, XU Yun, JIANG Ting-xue, DING Yun-hong, WANG Xiao-quan, LU Hai-bing. “Fracture network” fracturing technique for improving post-fracturing performance of low and ultra-low permeability reservoirs [J]. Acta Petrolei Sinica, 2009, 30(2): 237−241. (in Chinese)
[21] WENG Ding-wei, LEI Qun, XU Yun, LI Yang, LI De-qi, WANG Wei-xu. Network fracturing techniques and its application in the field [J]. Acta Petrolei Sinica, 2011, 32(2): 280−284. (in Chinese)
[22] WU Qi, XU Yun, WANG Xiao-quan, WANG Teng-fei, ZHANG Shou-liang. Volume fracturing technology of unconventional reservoirs: Connotation, optimization design and implementation [J]. Petroleum Exploration and Development, 2012, 39(3): 352−358. (in Chinese)
[23] WANG Yong-hui, LU Yong-jun, LI Yong-ping, WANG Xin, YAN Xue-mei, ZHANG Zhi-yong. Progress and application of hydraulic fracturing technology in unconventional reservoir [J]. Acta Petrolei Sinica, 2012, 33(S1): 149−158. (in Chinese)
[24] TANG Jun-wei, JIA Ai-lin, HE Dong-bo, WANG Wei-hong, FAN Li-hong, BAI Quan-ming, LIU Feng-zhen. Development technologies for the Sulige gas field with low permeability and strong heterogeneity [J]. Petroleum Exploration and Development, 2006, 33(1): 107−110. (in Chinese)
[25] YAO Xi-bin, GUO Xin-jiang. The geologic condition of gas accumulation and the key technology of exploration and exploitation of the deep tight sand gas reservoir of Xujiahe formation in the west Sichuan basin [J]. Sino-global Energy, 2012, 17(2): 43−50. (in Chinese)
[26] WARPINSKI N R, TEUFEL T W. Influence of geologic discontinuities on hydraulic fracture propagation [J]. JPT, 1987, 39(2): 209−220.
[27] BLANTON T L. Propagation of hydraulically and dynamically induced fractures in naturally fractured reservoirs [C]// The SPE Unconventional Gas Technology Symposium. Louisville: SPE, 1986: 613−621.
[28] ZHOU Jian, CHEN Mian, JIN Yan, ZHANG Guang-qing. Experimental study on propagation mechanism of hydraulic fracture in naturally fractured reservoir [J]. Acta Petrolei Sinica, 2007, 28(5): 109−113. (in Chinese)
[29] BEUGELSDIJK L J L, DEPATER C J, SATO K. Experimental hydraulic fracture propagation in a multi-fractured medium [C]// The SPE Asia Pacific Conference on Integrated Modeling for Asset Management. Yokohama: SPE, 2000: 177−184.
[30] WARPINSKI N R, BRANAGAN P T. Altered-stress fracture [C]// The SPE Rocky Mountain Regional Meeting. Casper: SPE, 1989: 990−996.
[31] CRANK J. The mathematics of diffusion [M]. Oxford: Oxford University Press, 1975.
[32] ZHAO Jin-zhou, REN Lan, HU Yong-quan. Controlling factors of hydraulic fractures extending into network in shale formations [J]. Journal of Southwest Petroleum University: Science & Technology Edition, 2013, 35(1): 1−9. (in Chinese)
[33] ZENG Lian-bo, GAO Chun-yu, QI Jia-fu, WANG Yong-kang, LI Liang, QU Xue-feng. Fracture distribution law and its seepage action of ultra-permeability sandstone reservoir in Longdong Area, Ordos Basin [J]. Scientia Sinica Terrae, 2008, 38(Supp.1): 41−47. (in Chinese)
[34] BULLER D, HUGHES S, MARKET J, PETRE E, SPAIN D, ODUMOSU T. Petrophysical evaluation for enhancing hydraulic stimulation in horizontal shale gas wells [C]// The SPE Annual Technical Conference and Exhibition. Florence: SPE, 2010: 431−451.
[35] SUN Hai-cheng, TANG Da-zhen. Shale gas formation fracture stimulation in the south Sichuan basin [J]. Journal of Jilin University: Earth Science Edition, 2011, 41(Sup.1): 34−68. (in Chinese)
[36] RICKMAN R, MULLEN M, PETRE E, GRIESER B, KUNDERT D. A practical use of shale petrophysics for stimulation design optimization: All shale plays are not clones of the Barnett shale [C]// The SPE Annual Technical Conference and Exhibition. Denver: SPE, 2008: 840−850.
[37] REN Fa-jun, JIA Hao-min, ZHANG Yao-gang, CAO Cheng-shou, WANG Ya-ling, LIU Lei. Hydraulic jetting perforation and segregated completion as a whole applied in the horizontal well drilling in the Jingbian gas field [J]. Natural Gas Industry, 2011, 31(10): 57−60. (in Chinese)
[38] LI Gen-sheng, XIA Qiang, HUANG Zhong-wei, TIAN Shou-ceng, SHENG Mao, QU Hong-na. Feasibility study and treatment design of hydrojet-fracturing in deep wells [J]. Petroleum Drilling Techniques, 2011, 39(5): 58−62. (in Chinese)
[39] CIPOLLA C L, WARPINSKI N R, MAYERHOFER M J, LOLON E P, VINCENT M C. The relationship between fracture complexity, reservoir properties, and fracture treatment design [C]// The SPE Annual Technical Conference and Exhibition. Denver: SPE, 2008: 2215−2239.
[40] PALISCH T T, VINCENT M C, HANDREN P J. Slickwater fracturing: Food for thought [C]// The SPE Annual Technical Conference and Exhibition. Denver: SPE, 2008: 1−20.

(Edited by DENG Lü-xiang)